

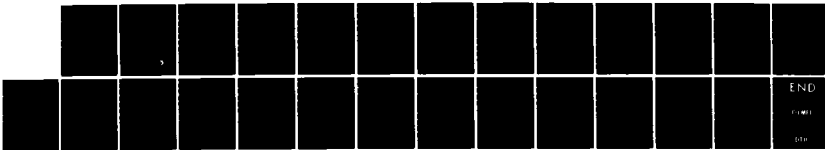
AD-A151 513 ON THE EFFECTS OF DELAMINATION DAMAGE IN FIBRE  
COMPOSITE LAMINATES(U) AERONAUTICAL RESEARCH LABS  
MELBOURNE (AUSTRALIA) R JONES ET AL. JUN 84

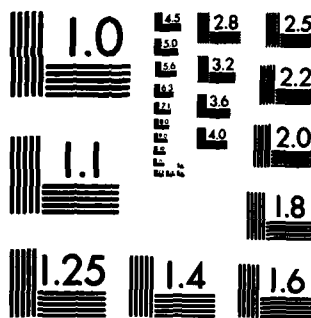
1/1

UNCLASSIFIED ARL-STRUC-R-403

F/G 11/4

NL





MICROCOPY RESOLUTION TEST CHART  
NATIONAL BUREAU OF STANDARDS-1963-A

ARL-STRUC-R-403/  
ARL-MAT-R-116

AR-003-927

2  
EPA



AD-A151 513

**DEPARTMENT OF DEFENCE  
DEFENCE SCIENCE AND TECHNOLOGY ORGANISATION  
AERONAUTICAL RESEARCH LABORATORIES  
MELBOURNE, VICTORIA**

**STRUCTURES REPORT 403 / MATERIALS REPORT 116**

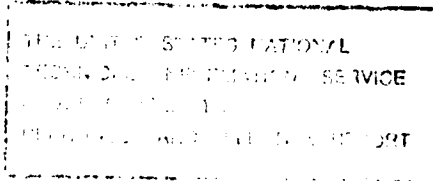
**ON THE EFFECTS OF DELAMINATION  
DAMAGE IN FIBRE COMPOSITE LAMINATES**

by

R. JONES, J. PAUL and W. BROUGHTON

DTIC FILE COPY

APPROVED FOR PUBLIC RELEASE



© COMMONWEALTH OF AUSTRALIA 1984 Commonwealth of Australia

1984  
C

JUNE 1984

COPY No

AR-003-927

DEPARTMENT OF DEFENCE  
AERONAUTICAL RESEARCH LABORATORIES  
DEFENCE SCIENCE AND TECHNOLOGY ORGANISATION

STRUCTURES REPORT 403 / MATERIALS REPORT 116

**ON THE EFFECTS OF DELAMINATION  
DAMAGE IN FIBRE COMPOSITE LAMINATES**

by

R. JONES, J. PAUL and W. BROUGHTON

**SUMMARY**

*This paper describes the results of a numerical investigation into the effects of delamination and impact damage on the compressive strength of graphite epoxy laminates and bonded metal-to-composite joints. For the laminates considered it is shown that as the size of the damage increases a stage is reached after which any further significant increase in the damage results in only a relatively small decrease in the residual compressive strength.*



© Commonwealth of Australia 1984

---

POSTAL ADDRESS: Director, Aeronautical Research Laboratories,  
Box 4331, P.O., Melbourne, Victoria, 3001, Australia

## CONTENTS

	Page No.
<b>NOTATION</b>	
<b>1. INTRODUCTION</b>	1
<b>2. LAMINATE CONFIGURATION</b>	1
<b>3. FINITE ELEMENT ANALYSIS</b>	1
<b>4. NUMERICAL RESULTS</b>	5
<b>5. DAMAGED STEP LAP JOINTS</b>	7
<b>6. CONCLUSION</b>	11
<b>7. REFERENCES</b>	
<b>APPENDIX</b>	
<b>DISTRIBUTION</b>	
<b>DOCUMENT CONTROL DATA</b>	

Accession For	
NTIS GRA&I	<input checked="" type="checkbox"/>
DTIC TAB	<input type="checkbox"/>
Unannounced	<input type="checkbox"/>
Justification	
By _____	
Distribution/ _____	
Availability Codes	
Dist	Avail and/or Special
A-1	



## NOTATION

$x, y, z$	Cartesian coordinates
$r, \theta, z$	Cylindrical polar coordinates
$\sigma_{ij}, \epsilon_{ij}$	Stress and strain components
$G$	Energy release rate
$J$	The $J$ integral
$K_1$	Mode 1 stress intensity factor
$\sigma_u$	Unnotched tensile strength
$d_0$	Critical damage zone size
$dw/dv$	Strain energy density
$r_c$	Critical core-zone size
$S$	Strain energy density factor
$\epsilon_f$	Far field failure strain

## 1. INTRODUCTION

Delamination damage in fibre composite materials may occur due to a variety of reasons, such as low energy impact or manufacturing defects. The presence of delamination damage is of major concern in the vicinity of bonded joints and in compressively loaded components where damage may grow under fatigue loading by out-of-plane distortion.

An early study into delamination growth arose from the B-1 composite development program [1]. This showed that delaminations can significantly reduce the fatigue life, and the residual compressive strength, for a compression dominated fatigue load spectrum. These effects have been confirmed in a series of recent articles [2, 3, 4, 5].

The present paper forms part of a joint investigation into delamination damage currently underway at both the Aeronautical Research Laboratories, Australia and the Royal Aircraft Establishment, England. In this work a three-dimensional finite element analysis is performed in order to understand the mechanisms involved in delamination growth, and subsequent failure, under compressive loading. This shows that as the size of damage increases a stage is reached after which any further increase in the damage produces only a relatively small decrease in the residual compressive strength.

## 2. LAMINATE CONFIGURATION

After examining the fracture surfaces of a quasi-isotropic laminate, which had failed under a compression fatigue spectrum, it was decided to test a series of laminates which contained a teflon disk between the second and third plies. The laminates were graphite epoxy with the following lay up:

- (i) Type A:  $(0/\pm 45/90)_{ss}$
- (ii) Type B:  $(0/\pm 45/90)_{4s}$
- (iii) Type C:  $(\pm 45/0/90/0)_{2s}$

The coupons constructed from laminate type A were 76.2 mm long, and 101.6 mm wide and contained a simulated delamination  $25.4 \text{ mm} \times 19.05 \text{ mm}$  between the 2nd and 3rd plies. The coupons constructed from laminate type B were 304.8 mm long and 101.6 mm wide with a delamination  $38.1 \text{ mm} \times 25.4 \text{ mm}$  in the same location. These two laminates were tested at the RAE and details of the experimental results can be found in [20].

The coupons constructed from laminate type C were 105 mm long and 45 mm wide and contained a variety of simulated delaminations and low-energy impact damage. These coupons were tested at ARL to determine the effect of the damage on the compressive strength of the laminate.

A detailed three-dimensional finite element analysis was performed on each set of coupon tests and the results of this investigation can be found in the following Sections.

## 3. FINITE ELEMENT ANALYSIS

The finite element analysis of complex three-dimensional delamination damage in laminated composites is particularly difficult. In general each ply must be modelled separately in order to obtain the correct values for the peel and the interlaminar shear stresses around the

delamination. In addition a fine mesh is required around the front of the delamination in order to correctly model the stress singularity. This results in a very large numerical model. In order to reduce the total number of degrees-of-freedom it is tempting to use eight-noded isoparametric bricks. Indeed this approach was used in [6, 7]. Unfortunately these elements cannot model the significant bending stresses which arise in the delamination problem [8]. Furthermore, since modelling is taking place at the ply level the elements have very large aspect ratios. This gives rise to problems of numerical ill-conditioning. Again, using the eight-noded bricks it is not possible to improve the conditioning of the problem. In general these elements should not be used with aspect ratios greater than five to one.

Consequently under no circumstances should eight-noded brick elements be used to model delamination problems in fibre composites.

The present investigation was done in double precision using twenty-noded isoparametric elements and a directionally reduced integration scheme with  $2 \times 2 \times 3$  Gaussian quadrature points, with 3 points being used through the thickness of the ply. This integration scheme is described in more detail in [9]. However, as mentioned above, if each ply is modelled separately the numerical model becomes excessively large and so a new super-element was developed.

In this paper the plies above the delamination are modelled separately as are the two plies below the delamination. The remaining plies are treated as a super element with the displacements varying quadratically in the local isoparametric coordinate system, as in Reissner thick-plate theory. With this approach the stiffness matrix for each super-element can still be written in the conventional form, viz.:

$$K = \iiint BDB^T dv \\ = \sum_{i=1}^N \iiint_{V_i} BD_i B^T dv \quad (1)$$

Here  $D_i$  is the elasticity matrix for the  $i$ th ply which has volume  $V_i$ .

There may be an arbitrary number of plies in a single super-element and thus unlike classical elements  $D$  varies throughout the thickness of the element. Details of the Gaussian quadrature required to integrate equation (1) correctly for an arbitrary number of plies is given in [9] and [10]. Such an approach significantly reduces the number of nodes and elements required and yet still allows for an accurate calculation of the stress field. However, even with this approach the problem consisted of six hundred of the twenty-noded isoparametric elements. As is now standard practice the mid-side nodes of the elements surrounding the delamination were moved to the quarter points in order to simulate the required singularity. It must be noted that when using eight-noded bricks as in [6, 7] it is not possible to represent the required stress singularity.

Having performed the stress analysis we must now decide on a criterion for assessing the severity of the delamination damage. Ideally we would like to evaluate the energy release rate  $G$ . This can be readily done for two-dimensional problems using either the method of virtual crack extension, as described in [11] for the edge delamination problem, or in the case of self-similar growth, by evaluating the  $J$  integral. For non self-similar growth  $J \neq G$ .

For problems which are not two dimensional there is no simple method for evaluating the energy release rate  $G$  without a prior knowledge of the way in which the delamination will grow. Furthermore whilst a line integral  $J_1^*$  has been developed [12], for three-dimensional fracture problems, this integral does not equal the true local energy release rate. This integral is defined by:

$$J_1^* = \lim_{\delta \rightarrow 0} \Phi \left( \frac{1}{2} \sigma_{ij} \frac{\partial u_i}{\partial x_j} \cdot \mathbf{i} - T_i \frac{\partial u_i}{\partial x_j} \right) ds \quad (2)$$

where the integration is along a contour of radius  $\rho$  normal to the front of the delamination. This integral coincides with the classical definition of  $J$  for 2-D problems, but for three-dimensional problems returns the local energy required for self-similar growth, i.e., circles into concentric circles, and not the true energy release rate. For metallic components under mode I fracture  $J_1^*$  is directly proportional to the local stress intensity factor  $K$ . Hence for metals  $J_1^*$  is a useful quantity. However, for our present problem the growth is mixed mode and non self-similar with the result that  $J_1^*$  is of questionable value.

Alternative approaches for assessing the severity of cracks and holes in fibre composite laminates have recently been developed [13, 14]. These methods are termed the point and average stress failure criteria. The point stress failure criterion assumes that failure will occur when the normal stress,  $\sigma_n$ , to the crack (or hole) at a distance  $d_o$  in front of the crack reaches the unnotched strength  $\sigma_u$  of the laminate, viz.:

$$\sigma_{n/x=d_o} = \sigma_u \quad (3)$$

The quantity  $d_o$  is usually called the damage zone size and for graphite epoxy laminates is typically 0.9 mm (=0.038").

The present paper uses the strain energy density approach [15, 16] to assess the delamination damage. This approach may be considered as an extension of the point stress failure criterion to allow for mixed mode failure.

Define the strain energy density in the usual fashion:

$$dw/dv = \frac{1}{2} \sigma_{ij} \epsilon_{ij} \quad (4)$$

Then for a two-dimensional problem the strain energy density approach has two basic hypotheses which apply for crack extension:

- (1) The crack will grow in the direction  $\theta = \theta_o$  of maximum potential energy density (viz.: minimum strain energy density).
- (2) Failure occurs when the stress field at a distance  $r_c$  ahead of the crack (or hole) in the direction  $\theta = \theta_o$  of the minimum strain energy density, is such that:

$$(dw/dv)_{\substack{r=r_c \\ \theta=\theta_o}} = (dw/dv)_c \quad (5)$$

Here  $(dw/dv)_c$  is the value, at failure of the strain energy density of the undamaged laminate. In this formulation  $r_c$  plays a similar role to  $d_o$ , the damage zone size used in the point stress failure formulation. Indeed as a first approximation we can take  $r_c \approx d_o$ . In this approach the strain energy density function  $S$  defined by

$$dw/dv = \frac{S}{r} + \text{higher order terms} \quad (6)$$

plays a central role. For mode I failure of orthotropic material  $S$  is proportional to the stress intensity factor  $K_1$ . Indeed the above hypothesis can be readily expressed in terms of  $S$ ; viz.:

Failure occurs in the direction  $\theta_o$  for which

$$\partial S / \partial \theta = 0 \text{ and } \partial^2 S / \partial \theta^2 > 0 \quad (7)$$

and when the load is such that

$$S/\theta = \theta_o = S_c \quad (=r_c (dw/dv)_c) \quad (8)$$

For three-dimensional damage we must first locate at each point along the damage front the local minimum of the strain energy density function  $S_{\min}(= r dw/dv_{\min})$ . Failure then initiates at the point along the front which has the maximum value of  $S_{\min}$ .

For incremental growth each point along the damage front advances a distance  $r$  which is determined from the relationship

$$\frac{S_1}{r_1} = \frac{S_2}{r_2} = \dots = \frac{S_i}{r_i} = \left( \frac{dw}{dv} \right)_c$$

A more detailed description of this hypothesis including its applicability to mixed mode crack growth can be found in [15, 16].

#### 4. NUMERICAL RESULTS

For the tests on laminates types A and B the finite element model yielded the maximum values of  $S_{min}$  along the lines  $AA'$  and  $BB'$ , see Figure 1. Indeed the values\* along these lines were relatively constant with the maximum value of  $S_{min}$  occurring at point  $D$ , approximately 3 mm below the centre line for specimens A and B. Specimen C, constructed from laminate type C, had the maximum value of  $S_{min}$  occurring exactly at the midsides of  $AA'$  and  $BB'$ .

The values of  $S^* = (S_{min})_{max}$  for laminates type A and B are given in Table 1 for a uniform compressive strain of 0.004 applied to the ends of the specimen.

TABLE 1

Values of  $S^*$

Laminate type	$S^*(\text{MPa.mm})$	$\epsilon_f$
A	0.0033	0.0061
B	0.0022	0.0075

In order to estimate the failure load we need the critical value of  $S$ , i.e.  $S_c$ . One early value of  $S_c$  for an epoxy was given as 0.055 lb/in ( $= 0.0096 \text{ MPa.mm}$ ), but more recent work [16] has found that a value of  $S_c = 0.044 \text{ lb/in}$  ( $= 0.0077 \text{ MPa.mm}$ ) is more representative. This value is for a Modulite II 5206 graphite epoxy.

Using this value for  $S_c$  and assuming that the coupon behaviour remains linear elastic we can now estimate the strain required to cause failure which we will denote as  $\epsilon_f$ . This value is given in Table 1.

It is particularly interesting to compare these predicted compressive failure strains with those given in [2] for a similar quasi-isotropic laminate with 32 plies, cf. laminate type B, and one with 24 plies; see Tables 2 and 3 respectively.

TABLE 2

Compressive failure strain  $\epsilon_f$  for a 32-ply quasi-isotropic laminate [from (2)]

$\epsilon_f$	Average Damage Area (mm)				
	426	523	587	671	929
0.0077	0.0075	0.0073	0.0067	0.0075	

\* The values of  $S$  were obtained via an interpolation procedure which is described in the Appendix.

TABLE 3

Compressive failure strain  $\epsilon_f$  for a 24-ply (0/45/0<sub>2</sub>/-45/0<sub>2</sub>/45/0<sub>2</sub>/-45/0)s laminate  
[from (2)]

$\epsilon_f$	Average Damage Area (mm)				
	458	574	645	703	955
	0.0060	0.0064	0.0057	0.0057	0.0060

As can be seen from Table 2 the failure strains predicted for laminate type B compare favourably with those measured in [2].

For the coupons constructed from laminates type C three different sizes of delaminations were modelled. The delaminated areas chosen were

- (a) 1" × 1" (25.4 mm × 25.4 mm)
- (b) 1" × 1½" (25.4 mm × 38.1 mm)
- (c) 1" × 2" (25.4 mm × 50.8 mm)

In each case the value of  $((dw/dv)_{min})_{max}$  occurred exactly at the centre of lines AA' and BB'. The corresponding values of  $S^* = (S_{min})_{max}$  for a compressive strain of 0.004 are shown in Table 4 along with the predicted values for  $\epsilon_f$  assuming as before that  $S_c = 0.044 \text{ lb/in}$  ( $= 0.0077 \text{ MPa.mm}$ ).

TABLE 4

	Delamination sizes (mm <sup>2</sup> )		
	645	967	1290
$S^*$ (MPa.mm)	0.0036	0.0034	0.0033
$\epsilon_f$	0.0057	0.0060	0.0061

Allowing for numerical error the value of  $S^*$ , and hence the failure strain  $\epsilon_f$ , remains fairly constant as the delamination size increases. This phenomenon can be seen to occur in the experimental results given in [2] and summarized in Tables 2 and 3. Indeed this can also be seen in the experimental results given in [4].

In the coupon tests on laminate C a number of 6.35 mm, 15.8 mm and 25.4 mm diameter inclusions were tested. These specimens failed at far-field strains of approximately 5200  $\mu$ , 5100  $\mu$  and 4980  $\mu$  respectively. Whilst there is a slight reduction in the far-field failure strain in going from the 6.35 mm diameter inclusion to the 25.4 mm diameter inclusion, this increase in area resulted in only a 5% decrease in strength.

In addition to this set of tests a second series of tests was performed on impact-damaged specimens. The failure strain  $\epsilon_f$  for these specimens is shown in Table 5.

TABLE 5  
Compressive strength of impact damaged specimens

	Damaged area (mm <sup>2</sup> )			
$\epsilon_f$	0·0	38	195	314
	0·0079	0·0067	0·0058	0·0049

It thus appears that as the size of the damaged area increases the value of  $S^*$  ( $= (S_{\min})_{\max}$ ) asymptotes to a constant value. As a result since failure occurs when  $S^* = S_c$  the residual strength also asymptotes to a constant level as the damage area increases.

It is important to note that this phenomenon has also been observed in the compressive strength of composite laminates containing edge delaminations [11, 17, 18, 19]. Although the present paper has used only small deformation theory in attempt to include large deformation effects is currently underway. Indeed recent analytical work\* by Professor D. C. Stouffer in the Department of Aerospace Engineering at the University of Cincinnati has shown that, even when large deformations occur, the energy release rate, and hence  $\epsilon_f$ , asymptotes to a constant value as the size of the delamination increases.

## 5. DAMAGED STEP-LAP JOINTS

Let us now examine the effect of delamination damage at a bonded step-lap joint. In order to understand the mechanisms involved a relatively simple joint configuration was considered; see Figure 2. The composite is a  $(\pm 45/02)_{2s}$  graphite epoxy with the delamination occurring at the interface between the titanium step and the 0 degree.

The moduli of the graphite epoxy were taken to be

$$G_{13} = G_{12} = G_{23} = 5 \cdot 0 \text{ GPa},$$

$$E_{22} = E_{33} = 9 \cdot 5 \text{ GPa},$$

$$E_{11} = 141 \text{ GPa},$$

$$\nu_{12} = \nu_{13} = 0 \cdot 31,$$

$$\nu_{23} = 0 \cdot 021.$$

The titanium was assumed to have  $E = 110 \text{ GPa}$  and  $\nu = 0 \cdot 3$ .

As before each ply was modelled separately using twenty-noded isoparametric bricks and the region around the crack front was modelled using the fifteen-noded isoparametric wedge elements with the mid points moved to the quarter points. A cross-section of the finite element mesh can be seen in Figure 3.

---

\* Private communication.

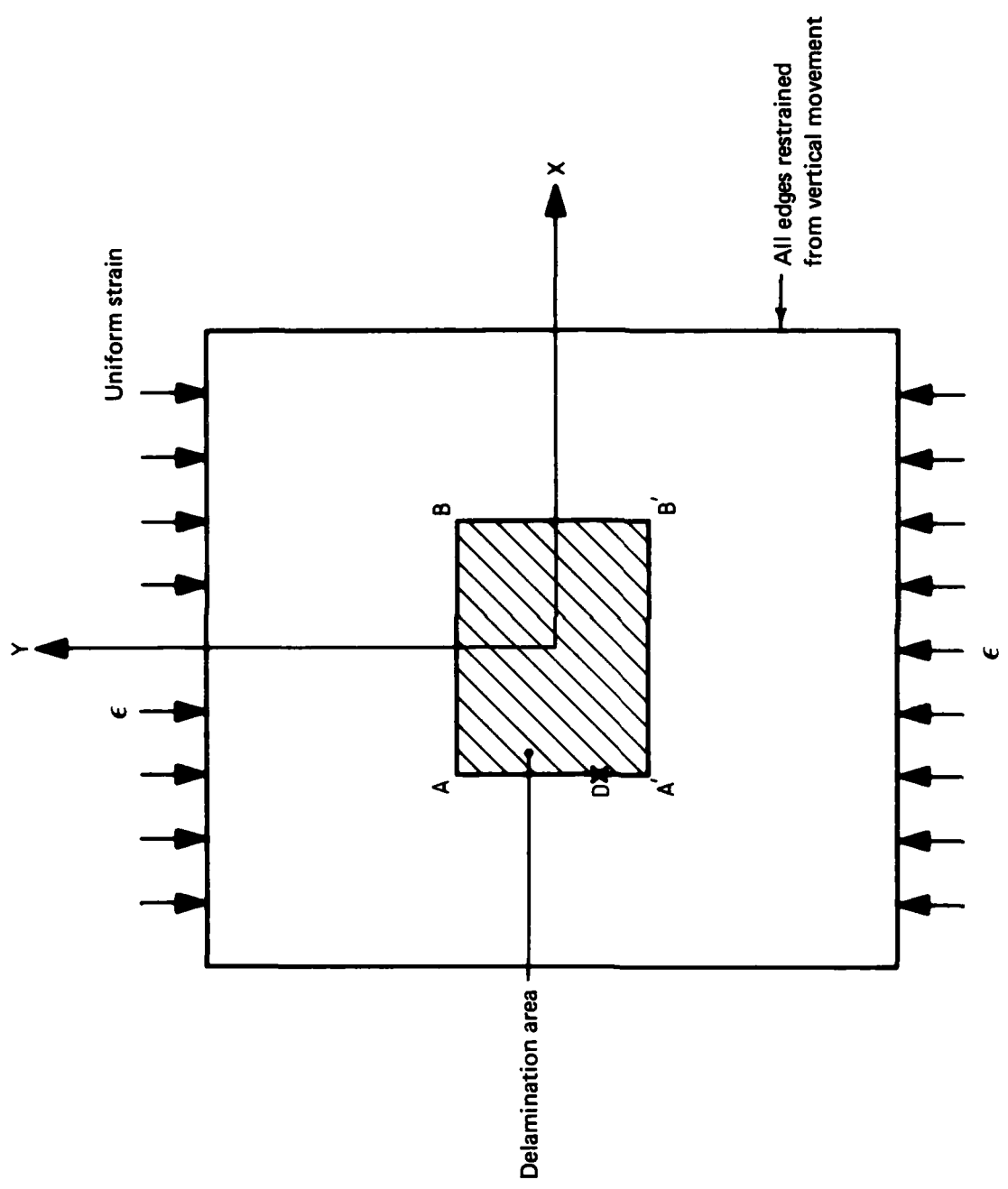


FIG. 1

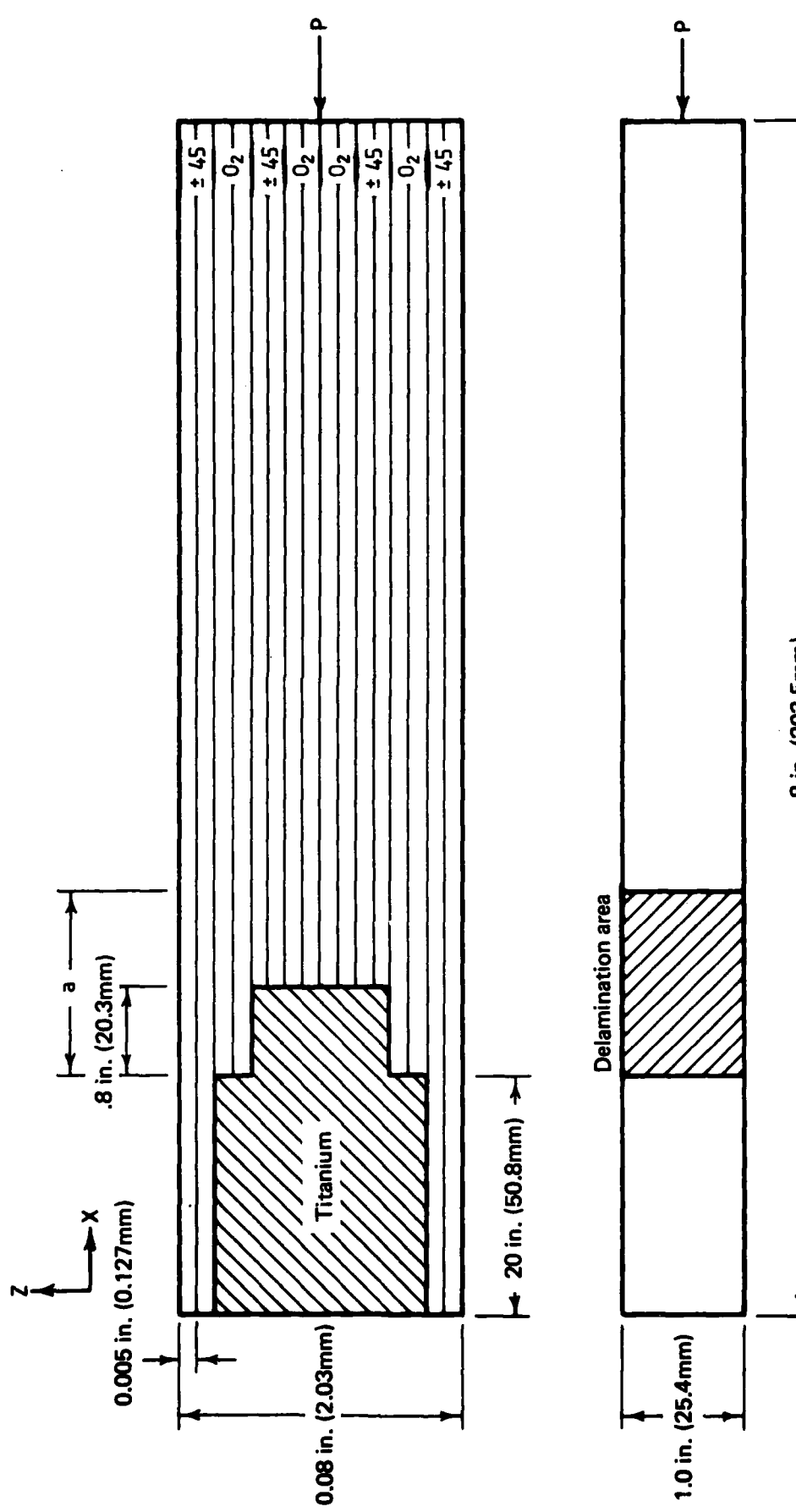


FIG. 2 PLY LAYUP AND DIMENSIONS

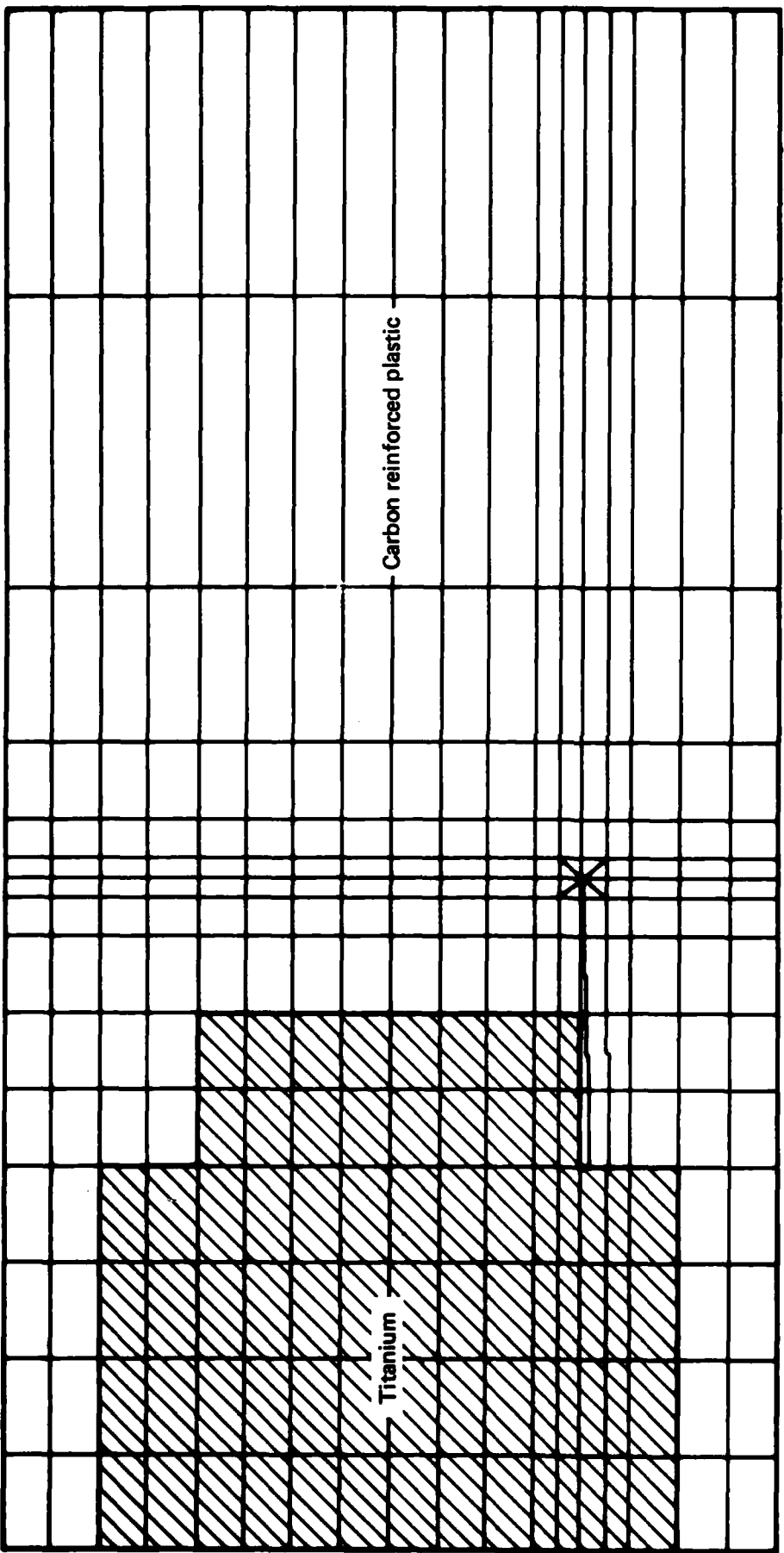


FIG 3 FINITE ELEMENT MESH X - SECTION

The delamination was found to close under applied compressive loading. As a result constraints were applied to the faces of the delamination so as to prevent the faces from crossing (i.e. overlapping). In this case the stresses and deformations were essentially two-dimensional so that the energy release rate  $G$  could be calculated from the relationship.

$$G = \frac{P^2}{2B} \frac{\partial \delta / P}{\partial a}$$

where  $P$  is the applied load  $B$  is the width of the specimen and  $\delta$  is the movement of the load point.

The values of  $G$  thus calculated are given in Table 6 for various size delaminations. These values correspond to an applied compressive strain of  $4000 \mu$ .

TABLE 6

	Delaminated area (mm <sup>2</sup> )					
	31·75	38·1	41·27	44·45	47·6	50·8
$G$ (MPa.mm)	0·0254	0·0284	0·029	0·0302	0·0314	0·0326

Here we see that going from a delamination of  $31\cdot75 \text{ mm}^2$  to  $50\cdot8 \text{ mm}^2$ , a  $60\%$  increase in the size of the damage, results in an increase in  $G$  of only  $28\%$ . This corresponds to a decrease in the residual strength of only  $13\%$ .

## 6. CONCLUSION

In this work we have found that for delamination damage, to both composite laminates and metal-to-composite joints, as the size of the damage increases a stage is reached after which any further significant increase in the damage produces only a small decrease in the residual compressive strength.

The next phase of this investigation involves detailed specimen testing in order to confirm the numerical results.

## 7. REFERENCES

1. Konishi, D. Y., and Johnston, W. R. Fatigue effects on delaminations and strength degradation in graphite-epoxy laminates, ASTM STP 674, p. 597, (1979).
2. Lauraitus, K. N., Ryder, J. T., and Pehit, D. E. Advanced residual strength degradation rate modelling for advanced composite structures, AFWAL-TR-79-3095, Volumes I and II, July 1981.
3. Rosenfeld, M. S., and Gause, L. W. Compression fatigue behaviour of graphite epoxy in the presence of stress raisers, ASTM STP 723, 174-196, (1981).
4. Stellbrink, K. K., and Aoki, R. M. Effect of defect on the behaviour of composites. Proc. Int. 4th Conf. Composite Materials, ICCM-IV Tokoyo 1982, pp 853-860.
5. Gause, L. W., Rosenfeld, M. S., and Vining, R. E. Effect of Impact damage on the XFU-12A composite wing box, 25th National SAMPE Symposium and Exhibition, Vol. 25, pp. 679-690 (1980).
6. Ratwani, M. M., and Kan, H. P. Compression fatigue analysis of fibre composites, J. Aircraft, Vol. 18, pp 458-462.
7. Ratwani, M. M., and Kan, H. P. Compression fatigue analysis of fibre composites, NADC-78049-60, September 1979.
8. Zienkiewicz, O. C. The finite element method, McGraw-Hill, 1982.
9. Jones, R., Teh, K. K., Callinan, R. J., and Brown, K. C. Analysis of multi-layer laminates using three-dimensional super elements, Int. J. Numerical Methods in Engng (in press).
10. Teh, K. K. A three-dimensional analysis of laminated composite plates using numerical methods, PhD Thesis, Melbourne University, June 1983.
11. Wang, A. S. D., and Crossman, F. W. Initiation and growth of transverse cracks and edge delamination in Composite laminates Part 1. An energy method J. Composite Material, 14, 72-87 (1980).
12. Blackburn, W. S., and Heller, T. K. Calculation of stress intensity factors in three dimensions by finite element methods. Int. J. Num. Methods in Engng, 11, 211-229 (1977).
13. Nuismer, R. J., and Whitney, J. M. Uniaxial failure of composite laminates containing stress concentrations, ASTM STP 593, pp 117-142, 1975.

14. Nuismer, R. J., and Labour, J. D. Application of the average stress failure criterion: Part 2—Compression, *J. Composite Material*, 13, January 1979.
15. Sih, G. C. *Mechanics of fracture 1: Methods of analysis and solutions of crack problems*, Noodhoff International Publishing, Leyden, pp 21–45 (1973).
16. Sih, G. C. *Mechanics of fracture 6: Cracks in composite materials*, Martinus Nijhoff Publishers, The Hague, pp XVI-LXXXI (1981).
17. Pei chi Chou, Wang, A. S. D., and Harry Miller. Cumulative damage model for advanced composite materials, *AFWAL-FR-82-4083*, September 1982.
18. Rybicki, E. F., Schueser, D. W., and Fox, J. An energy release rate approach for stable crack growth in free edge delamination problems, *J. Composite Materials*, 11, p. 470 (1977).
19. Wang, S. S. Edge delaminations in angle ply composite laminates, Final Report Part V, NASA CR 165439 (1981).
20. Jones, R., Broughton, W., Mousley, R. F., and Potter, R. T. Compression failures of damaged graphite epoxy laminates, *J. Composite Structures*, submitted March 1984.

## APPENDIX

Consider two points at distances  $r_1$  and  $r_2$ , such that  $r_1 > r_2$ , and which lie in a straight line in the direction of crack (i.e., delamination) growth. Both  $r_1$  and  $r_2$  are chosen to be much smaller than the crack length. In the present work we have also chosen  $r_1 = d_0 = 0.9$  mm ( $= 0.038''$ ). Then from equation (6) we see that

$$\left(\frac{dw}{dv}\right)_{r_1} - \left(\frac{dw}{dv}\right)_{r_2} = S\left(\frac{1}{r_1} - \frac{1}{r_2}\right) \quad (\text{A1})$$

which gives the value of  $S$  as

$$S = [(dw/dv)_{r_1} - (dw/dv)_{r_2}] / (1/r_1 - 1/r_2) \quad (\text{A2})$$

## DISTRIBUTION

### AUSTRALIA

#### DEPARTMENT OF DEFENCE

##### Central Office

Chief Defence Scientist  
Deputy Chief Defence Scientist  
Superintendent, Science and Program Administration  
Controller, External Relations, Projects and Analytical Studies } (1 copy)  
Defence Science Adviser (U.K.) (Doc. Data sheet only)  
Counsellor, Defence Science (U.S.A.) (Doc. Data sheet only)  
Defence Science Representative (Bangkok)  
Defence Central Library  
Document Exchange Centre, D.I.S.B. (18 copies)  
Joint Intelligence Organisation  
Librarian H Block, Victoria Barracks, Melbourne  
Director General—Army Development (NSO) (4 copies)

##### Aeronautical Research Laboratories

Director  
Library  
Superintendent—Structures  
Divisional File—Structures  
Authors: R. Jones  
J. Paul  
W. Broughton

##### Materials Research Laboratories

Director/Library

##### Defence Research Centre

Library

##### Navy Office

Navy Scientific Adviser  
Directorate of Naval Aircraft Engineering  
Superintendent, Aircraft Maintenance and Repair

##### Army Office

Army Scientific Adviser  
Engineering Development Establishment, Library  
US Army Research, Development and Standardisation Group

### **Air Force Office**

Air Force Scientific Adviser  
Technical Division Library  
Director General Aircraft Engineering—Air Force  
HQ Operational Command (SMAINTSO)  
HQ Support Command (SLENGO)

### **DEPARTMENT OF DEFENCE SUPPORT**

#### **Government Aircraft Factories**

Library

### **DEPARTMENT OF AVIATION**

Library  
Flying Operations and Airworthiness Division

### **STATUTORY AND STATE AUTHORITIES AND INDUSTRY**

CSIRO, Materials Science Division, Library  
Trans-Australia Airlines, Library  
Ansett Airlines of Australia, Library  
Commonwealth Aircraft Corporation, Library  
Hawker de Havilland Aust. Pty Ltd, Bankstown, Library

### **UNIVERSITIES AND COLLEGES**

Adelaide	Barr Smith Library
Flinders	Library
Latrobe	Library
Melbourne	Engineering Library
Monash	Hargrave Library
Newcastle	Professor I. J. Polmear, Materials Engineering Library
Sydney	Engineering Library
N.S.W.	Physical Sciences Library Professor R. A. A. Bryant, Mechanical Engineering Assoc. Professor R. W. Traill-Nash, Civil Engineering
Queensland	Library
Tasmania	Engineering Library
Western Australia	Library
R.M.I.T.	Library Dr H. Kowalski, Mech. & Production Engineering

**CANADA**

CAARC Coordinator Structures  
NRC  
Aeronautical and Mechanical Engineering Library

**Universities and Colleges**

Toronto              Institute for Aerospace Studies

**FRANCE**

ONERA, Library

**INDIA**

CAARC Coordinator Structures  
Defence Ministry, Aero Development Establishment, Library  
Hindustan Aeronautics Ltd, Library  
National Aeronautical Laboratory, Information Centre

**INTERNATIONAL COMMITTEE ON AERONAUTICAL FATIGUE**

Per Australian ICAF Representative (25 copies)

**ISRAEL**

Technion-Israel Institute of Technology  
Professor J. Singer

**JAPAN**

National Research Institute for Metals, Fatigue Testing Division

**Universities**

Kagawa University    Professor H. Ishikawa

**NETHERLANDS**

National Aerospace Laboratory (NLR), Library

## **NEW ZEALAND**

Defence Scientific Establishment, Library

## **SWEDEN**

Swedish National Defence Research Institute (FOA)

## **SWITZERLAND**

F+W (Swiss Federal Aircraft Factory)

## **UNITED KINGDOM**

Ministry of Defence, Research, Materials and Collaboration  
CAARC, Secretary  
Royal Aircraft Establishment  
    Farnborough, Dr G. Wood, Materials Department  
Commonwealth Air Transport Council Secretariat  
Admiralty Marine Technology Establishment  
    Holton Heath, Dr N. J. Wadsworth  
St Leonard's Hill, Superintendent  
National Physical Laboratory, Library  
National Engineering Laboratory, Library  
British Library, Lending Division  
CAARC Coordinator, Structures

### **Universities and Colleges**

Bristol	Engineering Library
Nottingham	Science Library
Southampton	Library
Strathclyde	Library
Cranfield Institute of Technology	Library
Imperial College	Aeronautics Library

## **UNITED STATES OF AMERICA**

NASA Scientific and Technical Information Facility  
Metals Information

**Boeing Company**  
Mr W. E. Binz  
Mr J. C. McMillan  
**Lockheed-California Company**  
**Lockheed Missiles and Space Company**  
**Lockheed Georgia**  
**McDonnell Aircraft Company, Library**  
**Applied Mechanics Reviews**

**Universities and Colleges**

Iowa	Professor R. I. Stephens
Illinois	Professor D. C. Drucker
Massachusetts Inst. of Technology	M.I.T. Libraries
Lehigh	Institute of Fracture and Solid Mechanics Professor G. C. Sih

**SPARES (20 copies)**

**TOTAL (160 copies)**

**Department of Defence**  
**DOCUMENT CONTROL DATA**

I. a. AR No. AR-003-927	I. b. Establishment No. ARL-STRUC-R-403/ ARL-MAT-R-116	2. Document Date June 1984	3. Task No. AIR 80/126
4. Title <b>ON THE EFFECTS OF DELAMINATION DAMAGE IN FIBRE COMPOSITE LAMINATES</b>		5. Security a. document Unclassified b. title      c. abstract U            U	6. No. Pages 14
8. Author(s) R. Jones, J. Paul and W. Broughton		9. Downgrading Instructions	
10. Corporate Author and Address Aeronautical Research Laboratories P.O. Box 4331, Melbourne, Victoria, 3001		11. Authority (as appropriate) a. Sponsor      c. Downgrading b. Security      d. Approval (a) AIR 80/126 (b) Dept. of Defence (Air Force Office)	
12. Secondary Distribution (of this document) Approved for public release.			
Overseas enquirers outside stated limitations should be referred through ASDIS, Defence Information Services Branch, Department of Defence, Campbell Park, CANBERRA, ACT, 2601.			
13. a. This document may be ANNOUNCED in catalogues and awareness services available to ... No limitations.			
13. b. Citation for other purposes (i.e. casual announcement) may be (select) unrestricted (or) as for 13 a.			
14. Descriptors Damage Delaminating Fibre composites Fibre laminates		15. COSATI Group 11040 11130	
16. Abstract <i>This paper describes the results of a numerical investigation into the effects of delamination and impact damage on the compressive strength of graphite epoxy laminates and bonded metal-to-composite joints. For the laminates considered it is shown that, as the size of the damage increases, a stage is reached after which any further significant increase in the damage results in only a relatively small decrease in the residual compressive strength.</i>			

This page is to be used to record information which is required by the Establishment for its own use but which will not be added to the DISTIS data base unless specifically requested.

**16. Abstract (Contd)**

**17. Imprint**  
Aeronautical Research Laboratories, Melbourne.

<b>18. Document Series and Number</b>	<b>19. Cost Code</b>	<b>20. Type of Report and Period Covered</b>
Structures Report 403/ Materials Report 116	214705	—

**21. Computer Programs Used**

**22. Establishment File Ref(s)**

**END**

**FILMED**

**4-85**

**DTIC**